Montmorillonite Functionalized with Pralidoxime As a Material for Chemical Protection against Organophosphorous Compounds

ARTICLE *in* ACS APPLIED MATERIALS & INTERFACES · MARCH 2011

Impact Factor: 6.72 · DOI: 10.1021/am200041e · Source: PubMed

ACS APPLIED MATERIALS & INTERFACES

RESEARCH ARTICLE

www.acsami.org

Montmorillonite Functionalized with Pralidoxime As a Material for Chemical Protection against Organophosphorous Compounds

Lev Bromberg,[†] Christine M. Straut,[‡] Andrea Centrone,[†,§] Eugene Wilusz,[⊥] and T. Alan Hatton*[,†]

[†]Department of Chemical Engineering, Massachusetts Institute of Technology, Cambridge, Massachusetts 02139, United States

[‡]Battelle Natick Operations, Natick, Massachusetts 01760, United States

[⊥]U.S. Army Natick Soldier Research, Development & Engineering Center, Materials and Defense Sciences Division, Natick, Massachusetts 01760, United States

Supporting Information

ABSTRACT: Montmorillonite K-10 functionalized with α-nucleophilic 2-pralidoxime (PAM) and its zwitterionic oximate form (PAMNa) is introduced as a versatile material for chemical protection against organophosphorous (OP) compounds such as pesticides and chemical warfare agents (CWA). Upon inclusion into the montmorillonite interlayer structure, the pyridinium group of PAMNa is strongly physisorbed onto acidic sites of the clay, leading to shrinking of the interplanar distance. Degradation of diethyl parathion by PAMNa-functionalized montmorillonite in aqueous-acetonitrile solutions occurred primarily via hydrolytic conversion of parathion into diethylthio phosphoric acid, with the initial stages of hydrolysis observed to be pseudo-first-order reactions. Hydrolysis catalyzed by the clay intercalated by PAMNa was 10- and 17-fold more rapid than corresponding spontaneous processes measured at 25 and 70 °C, respectively. Hydrolytic degradation of diisopropyl fluorophosphate (DFP), a CWA simulant, was studied on montmorillonite clay functionalized by PAMNa and equilibrated with water vapor at 100% relative humidity by ^{31}P high-resolution magic angle spinning NMR and was observed to be rather facile compared with the untreated montmorillonite, which did not show any DFP hydrolysis within 24 h. The incorporation of the functionalized clay particles into elastomeric film of polyisobutylene was shown to be a means to impart DFP-degrading capability to the film, with clay particle content exceeding 18 wt %.

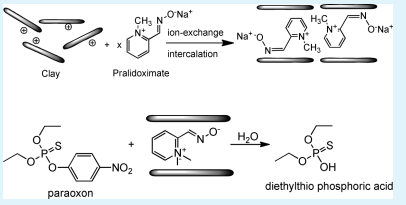

KEYWORDS: montmorillonite K-10, pyridine-2-aldoxime methiodide, functionalization, organophosphate hydrolysis, protective barrier

INTRODUCTION

Large specific surface area, chemical and mechanical stability, layered structure, and high cation exchange capacity have made clays excellent adsorbent materials as well as useful components of barrier protective materials because of the existence of several types of active sites on their surface, including Brønsted and Lewis acids, and ion exchange sites.[1] Montmorillonite clay is composed of units made up of two silica tetrahedral sheets with a central alumina octahedral sheet. The formula for montmorillonite is $(Si_{7.8}Al_{0.2})^{IV}(Al_{3.4}\,Mg_{0.6})^{VI}O_{20}(OH)_4$ and the theoretical composition without the interlayer material is SiO_2, 66.7%; Al_2O_3, 28.3%; H_2O, 5%. Montmorillonite typically consists of layered structures with strong intralayer bonds and relatively weak interlayer interactions and possesses a net negative charge of 0.8 per unit cell, and this has been responsible for giving superior activity to montmorillonite as an adsorbent. The structure of montmorillonite is affected by its exposure to water and aqueous solutions of small organic compounds. Hence, many organic molecules with polar functional groups, ions, and water molecules hydrating the ions can be intercalated in the interlayer space of montmorillonite, producing swelling (expansion of the distances between basal planes).[2−4] The adsorption mechanism of polar molecules most frequently implied is via ion−dipole forces.[5,6]

It is well-known that clays such as montmorillonite and kaolinite accelerate the degradation of insecticides such as chlorpyrifos, paraoxon and methyl and ethyl parathions.[8−12] Such degradation can be primarily attributed to the dissociative or destructive chemisorption processes occurring on clays containing interlayer metal (M) cations that display significant acidity due to the hydroxo species formed through deprotonation of coordinated water molecules[13]

$$[M(OH_2)_n]^{m+} \rightarrow [M(OH_2)_{n-1}OH]^{(m-1)+} + H^+$$

The metal hydroxo species can serve as nucleophiles that are stronger than H_2O.[14] Like other nucleophiles containing an atom with an unshared pair of electrons adjacent to the reaction site, oximate bases are known to exhibit a much higher reactivity than common oxyanionic nucleophiles of similar basicities in many substitution processes, a phenomenon known as the alpha-effect.[15] It is interesting to note that the literature on activity of clays modified by α-nucleophiles such as oximates is lacking,

Received: January 12, 2011
Accepted: March 25, 2011
Published: March 25, 2011

dx.doi.org/10.1021/am200041e | ACS Appl. Mater. Interfaces 2011, 3, 1479–1484

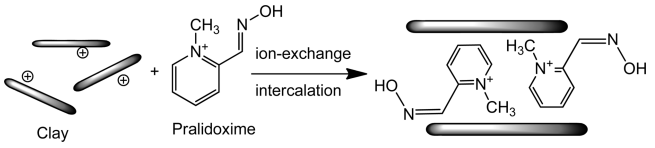

Figure 1. Functionalization of montmorillonite K-10 with PAM via ion-exchange of the clay's cations for PAM cations.

despite ~~of~~ the intuitively expected synergistic effect of the α-nucleophile "added" to the already nucleophilic clay.

In the present work, we aimed at highly reactive, nucleophilic clay particles as components of reactive barrier materials, and thus pralidoxime (pyridine aldoxime methiodide, or PAM) was our cationic compound of choice. PAM was originally designed as a highly efficient antidote that binds to organophosphate-inactivated acetylcholinesterase. It is used by the military to combat poisoning by acetylcholinesterase inhibitors (nerve agents). We have previously observed a high activity of PAM in hydrolysis of diisopropyl fluorophosphate (DFP).[16] Molecules like PAM and PAMNa can be introduced into the interlayer space of montmorillonite, affecting its structure depending on the density of the layer charge, the degree of exchange, and the host−guest and guest−guest interaction energy. This motivated the use of PAM as the choice for the clay particle modification. A cartoon illustrating PAM inclusion into montmorillonite is shown in Figure.1.

The PAM-modified montmorillonite appears to be reactive toward toxic organosphosphates, as described below.

EXPERIMENTAL SECTION

Materials. Montmorillonite K-10, diethyl paraoxon (99%), pyridine-2-aldoxime methiodide (98%), sodium methoxide (≥97%) and diisopropyl fluorophosphate (DFP, 99%) were received from Sigma-Aldrich Chemical Co. and polyisobutylene (PIB, viscosity average molecular weight 850,000) was obtained from Scientific Polymer Products, Inc. Montmorillonite K-10, an acidic clay purchased from Aldrich possesses BET surface area of 220 m^2/g and the following chemical composition (average value): SiO_2 (73.0%), Al_2O_3 (14.0%), Fe_2O_3 (2.7%), CaO (0.2%), MgO (1.1%), Na_2O (0.6%), K_2O (1.9%).[17]

Prior to the use, a fraction of PAM was converted to pralidoximate (PAMNa) by dissolving PAM in deionized water at 10 mg/mL while adjusting the pH to 8.6 by adding minute quantities of sodium methoxide, followed by lyophilization of the resulting solution. All other chemicals and solvents were obtained from commercial sources and were of the highest purity available.

Syntheses. The montmorillonite K-10 (MMNK-10) was functionalized by pralidoxime methiodide (PAM) at room temperature as follows. PAM was dissolved in deionized water at 10 wt % concentration after pH adjustment to 8.6 using sodium methoxide. One gram of sodium montmorillonite was added to the solution and the suspension was shaken at 250 rpm overnight. The montmorillonite particles were removed from the suspension by centrifugation (6,000 *g*, 15 min), snap-frozen in liquid nitrogen and lyophilized to dryness. The pH of the solution equilibrated with the montmorillonite was 8.6.

Elastomeric films were made by casting 10 wt % solution of PIB in toluene over a Teflon surface followed by brief drying at 70 °C and then at 25 °C under vacuum until constant weight. Prior to casting, a weighed amount of montmorillonite or functionalized montmorillonite particles was added to a 1.0 g of PIB/toluene solution. The resulting paste was vigorously stirred using a spatula for 1−2 min and then spread over a Teflon sheet surface (~10 × 5 cm) and dried.

Methods. XRD measurements were recorded with a PANalytical X'Pert PRO diffractometer (PANalytical B.V., Almelo, The Netherlands) equipped with an X'celerator linear detector using a CuKα radiation source. Samples were prepared as thin powder layers over zero-background plates, and progressive slits were used to illuminate a constant length of the samples (5 mm). XRD patterns were acquired over 18 h in the range of 2 to 65° 2θ using a nickel filter or a monochromator. Unit cell parameters were determined using Jade software (Jade Software Co., San Pedro, CA) with empirical peak profile fitting.

FTIR spectroscopy was performed on a NEXUS 870 FTIR spectrometer (Thermo Nicolet Inc.). Spectra were recorded over the wavenumber range between 4000 and 400 cm^{-1} at a resolution of 2 cm^{-1} and are reported as the average of 64 spectral scans. All samples were dried under vacuum to constant weight, ground and blended with KBr, and pressed to form the pellets used in the measurements. Thermogravimetric analysis (TGA) was conducted using a Q5000IR thermogravimetric analyzer (TA Instruments, Inc.). Samples were subjected to heating scans (20 °C/min) in a temperature ramp mode.

The kinetics of diethyl parathion degradation were studied in 4 mg/mL suspensions of the montmorillonite species suspended in monophasic solutions of parathion (6.5 mM) in acetonitrile and 50 mM solution of N-cyclohexyl-2-aminoethanesulfonic acid (CHES) in deuterium oxide (pD 8.6). The concentration of the aqueous (D_2O) buffer in acetonitrile was 27 wt % and was optimized to 1) enable monophasic solutions of water-insoluble parathion, 2) maintain pH throughout the reaction, and 3) enable proper locking of the NMR signals. The montmorillonite samples were suspended in the acetonitrile/buffer solutions and kept at 25 or 70 °C with periodic vortexing and brief sonication for proper mixing. Kinetics of parathion degradation in suspensions were assessed by liquid state ^{31}P NMR spectrometry using a Bruker Avance 400 spectrometer operating at 161.98 MHz. At $t = 0$, an aliquot of parathion solution in acetonitrile was added to the clay suspension nas above and the experiment commenced. At given time intervals, the top clear solution (0.7 mL) was carefully withdrawn from the suspension by a pipet and placed into an NMR tube. The spectra were recorded by accumulation of 200 scans. The solution was placed back into the suspension immediately after each NMR measurement. The degree of parathion conversion was expressed as $F_t = \Sigma I_p/(\Sigma I_r + \Sigma I_p)$, where ΣI_r and ΣI_p are the sums of the integrations of the signals corresponding to the reactant (parathion, 62.4 ppm) and the products.The observed rate constant, k_{obs}, is found from the slope of the $\ln(1 - F_t)$ vs t plot[18]

$$\ln(1 - F_t) = -k_{obs}t \quad (1)$$

Measurement of DFP degradation was performed on 20−55 mg of MMNK-10 clay, functionalized clay, and on polyisobutylene rubber modified with intercalated MMNK-10 clay. The tested materials were equilibrated for 1 week at 100% relative humidity in a sealed chamber equipped with a water bath. High-resolution magic angle spinning (HRMAS) ^{31}P spectroscopy was performed on a Bruker Avance 400 spectrometer operating at 161.98 MHz. Spectra were recorded with a 4-mm ^{31}P gradient probe at a temperature of 20 °C using standard Bruker software sequences. The measurement parameters were: MAS rate, 5 kHz; pulse, 90°; pulse width, 6 μs; acquisition time, 5 min. Tested sample was placed in a weighed NMR rotor (sample volume, 50 μL) and 2 μL of DFP liquid were applied to the top surface of the packed sample using a syringe. During each measurement, three main signals were monitored (see Figure S-2 in the Supporting Information); doublets at 3.7 and 9.7 ppm coupled by the P−F bond ($J_{P-F} \approx 970$ Hz) are assigned to the reactant DFP, whereas the signal at ~17 ppm corresponds to the degradation product (diisopropyl phosphoric acid).[19] The hydrolysis rate was calculated according to eq 1.

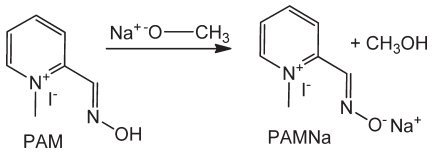

Figure 2. Synthesis of pralidoxime from PAM.

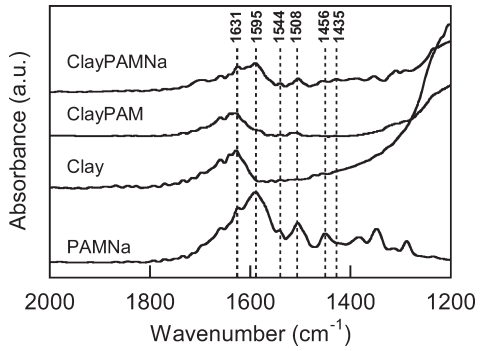

Figure 3. FTIR spectra of PAMNa and untreated (Clay) and functionalized (ClayPAM, ClayPAMNa) montmorillonite K-10.

RESULTS AND DISCUSSION

Material Characterization. In the present work, we explored a concept of utilizing α-nucleophilic properties of 2-pyridine aldoxime methyl iodide (PAM) to create protective materials capable of degradation of organophosphorous compounds mimicking CWA. PAM and other oximes act as strong nucleophiles in deacylation and dephosphorylation of esters, and their efficiency in dephosphorylation can be enhanced by conversion into corresponding oximate anions, which in the case of PAM should be termed zwitterions (Figure 2)[16,20,21]

Reactivity of the oximates can suffer a saturation effect and decay with increasing basicity in aqueous solution above a pH of 9,[20] and thus we performed the conversion of PAM to PAMNa at pH 8.6, i.e., just above the pK_a value of 8.23 reported for PAM.[22] As reported below, PAM converted to the PAMNa form possessed a higher reactivity toward the OP compounds studied. It should be noted that upon reaching pH 8.6 in the aqueous solution of PAM in the process of the solution titration with minute quantities of sodium methoxide, the solution was snap-frozen in liquid nitrogen and dried under high vacuum, in a procedure designed to arrest possible degradation effects that are known to occur in aqueous alkaline solutions of PAM at elevated temperatures.[23] No residual methanol or methoxide was observed in thus prepared PAMNa by ^{1}H NMR (see Figure S-3 in the Supporting Information). Functionalization of the montmorillonite K-10 (MMNK-10) was consequently performed by suspending the clay particles in aqueous solutions of PAM and PAMNa at pH 3.2 and 8.6, respectively, resulting in two distinct species of functionalized clays, which we term ClayPAM and ClayPAMNa, respectively, in what follows.

Figure 3 shows the ring-stretching region of the FTIR spectra of the untreated MMNK-10 clay, PAMNa, and MMNK-10 clay functionalized with PAMNa (pH 8.6) and (pH 3.2). The band at 1631 cm^{-1} due to H—O—H stretching vibrations[24,25] is observed both in the untreated and functionalized clays. The absorption bands at 1544, 1508, and 1456 cm^{-1} correspond to Brønsted, both Brønsted and Lewis, and Lewis acidic moieties of the montmorillonite, respectively, interacting with the positively charged methylpyridinium moiety of PAM.[17,25,16] The pyridinium group of PAMNa physisorbed onto clay shows bands at 1595 and 1435 cm^{-1}. Interestingly, the intensity of the band at 1595 cm^{-1} is greatly reduced in the spectrum of MMNK-10 modified with PAM at pH 3.2, indicating much weaker interaction compared with the case of modification at pH 8.6, where PAM exists in the zwitterionic oximate form (Figure 2).

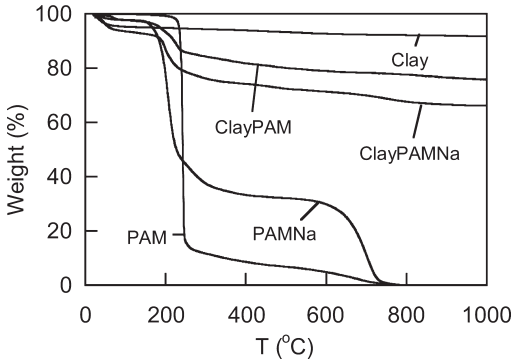

Figure 4. Thermogravimetric analysis of pralidoxime (PAM), pralidoximate (PAMNa), montmorillonite K-10 untreated (Clay) and functionalized by pralidoxime at pH 3.2 (ClayPAM) or pH 8.6 (ClayPAMNa).

TGA thermograms of the montmorillonite K-10 (MMNK-10), functionalized MMNK-10 and PAM and its oximate form, PAMNa are shown in Figure 4. The thermogram of PAM methiodide recrystallized from hot water at pH 3.2 exhibits a sharp melting-decomposition transition at 225 °C, in accordance with the supplier's data. It is interesting to observe that the same compound dissolved in aqueous solution of sodium methoxide at pH 8.6 and lyophilized (PAMNa) demonstrated a significantly different thermogram. The PAMNa lost approximately 10 wt % upon heating to 90 °C and then showed two broad decomposition processes at >135° and above 600 °C, which may be an indication of the presence of hydrates and PAM crystal polymorphs.

As-received and dried under a vacuum at 25 °C MMNK-10 still contained approximately 5% of water removed by thermal dehydration at 105 °C, which is in excellent agreement with the reported hydration water content of 4.9 wt % in pristine MMNK-10;[26] this value is slightly smaller than the water content of 6.7 wt % that can be deduced from the reported total cation-exchange capacity of MMNK-10 of 0.963 mol/kg,[27] with the assumption of four hydration water molecules per ion.[28] MMNK-10 functionalized with PAM contained approximately 3 and 6 wt % of hydrate water in the case of ClayPAM and ClayPAMNa, respectively. In the 180—220 °C temperature range, functionalized MMNK-10 samples showed a sharp degradation process, followed by broad weight loss up to 1000 °C, at which point the residual weight of the samples was 76 and 66 wt % in the case of ClayPAM and ClayPAMNa, respectively. These measurements enabled estimation of the oxime/oximate species content in the functionalized samples to be 21 wt % (0.80 mol/kg) and 28 wt % (0.98 mol/kg) for the MMNK-10 clay loaded with PAM and PAMNa, respectively. In the calculations, we assumed the molecular mass of the loaded species to be 264.06 Da (2-[(hydroxyimino)methyl]-1-methylpyridinium iodide) and 286.05 Da (sodium salt of PAM oximate, see Figure 2). The estimate obtained for PAMNa (0.98 mol/kg) corresponded well

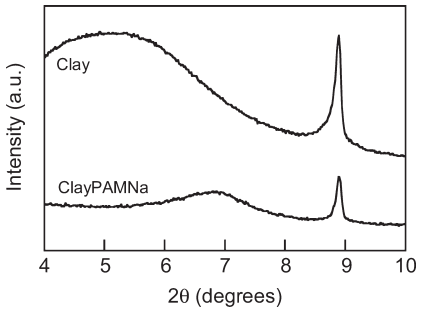

Figure 5. Typical X-ray diffraction patterns of untreated MMNK-10 (Clay) and MMNK-10 clay functionalized with PAMNa at pH 8.6 (ClayPAMNa).

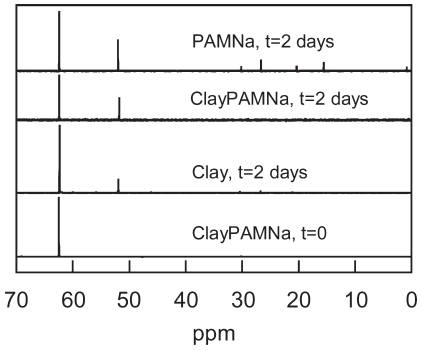

Figure 6. Typical ^{31}P NMR spectra of parathion degradation at pD 8.6, 70 °C and time points taken at t = 0 or 2 days. Solvent: 50 mM CHES/D_2O buffer (27 wt %, pD 8.6) in acetonitrile. Initial concentration of parathion, 6.5 mM. Hydrolytic species are added at 4 mg/mL concentrations. Designations: Clay (montmorillonite K-10), ClayPAMNa (montmorillonite K-10 functionalized by sodium pralidoxime, pH 8.6), PAMNa (pralidoxime methiodide obtained by freeze-drying PAM solution with pH adjusted to 8.6 by sodium methoxide). At t = 0, identical spectra without the hydrolysis products were observed in the presence or absence of functionalized clays or PAMNa (not shown for clarity).

with the total cation exchange capacity of the MMNK-10 for a total cation-exchange capacity of MMNK-10 reported to be 0.963 mol/kg.[27] As discussed below, the obtained "payload" values of the studied clays enabled estimation of the comparative rate constants of the PAM compounds in their heterogeneous reactions with organophosphorous esters.

The TGA results can be related to the XRD patterns depicted in Figure 5. The untreated MMNK-10 shows a basal spacing of 0.99 nm at 2θ = 8.89° and a reflection peak at 2θ = 6.22°, corresponding to a distance of 1.42 nm, which is attributed to a majority of the interlayer spaces being intercalated with water molecules.[29] Adsorption of PAMNa onto MMNK-10 leads to a shrinking of the basal planar distance to 1.27 nm corresponding to 2θ = 6.90°. Analogous changes were observed with PAM adsorbed from a solution at pH 3.2, whereas treatment of the MMNK-10 with an aqueous solution of sodium methoxide (pH 8.6) followed by drying under vacuum resulted in partial dissolution of the clay and disappearance of the d_{001} peak (see Figure S-1 in the Supporting Information). The lower interplanar distance after PAM or PAMNa adsorption indicates the successful intercalation of these compounds, which displace the intercalated water molecules from the interlayer spaces. This phenomenon is

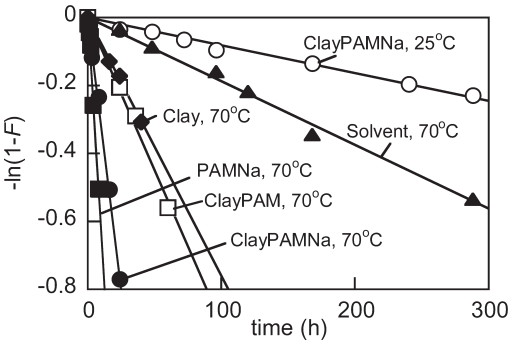

Figure 7. Typical kinetics of parathion hydrolysis at pD 8.6 and T = 25 or 70 °C. Solvent: 50 mM CHES/D_2O buffer (27 wt %) in acetonitrile. Initial concentration of parathion, 6.5 mM. Hydrolytic species designations: Clay (montmorillonite K-10), ClayPAM (montmorillonite K-10 functionalized with pralidoxime methiodide, pH 3.2), ClayPAMNa (montmorillonite K-10 functionalized with pralidoxime methiodide, pH 8.6), PAMNa (pralidoxime methiodide obtained by drying pralidoxime methiodide solution with pH adjusted to 8.6 by sodium methoxide).

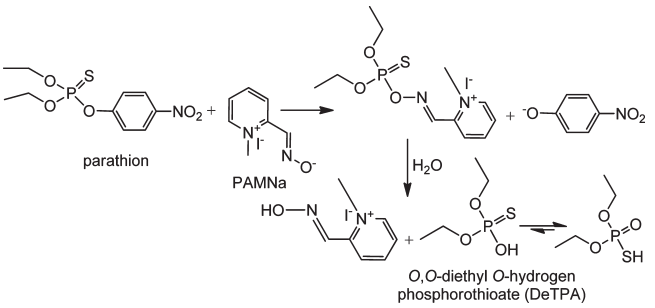

Figure 8. Predominant pathway of the nucleophilic hydrolysis of parathion in the presence of PAMNa nucleophile.

typically observed after the absorption of organic cations from water solutions onto clays.[2,30]

Parathion Degradation. The effect of functionalzation of montmorillonite K-10 with PAM on the hydrolysis of the insecticide parathion was explored to access the potential of the modified clay as a material for chemical protection.

Parathion is quite stable in aqueous media at ambient temperatures. For instance, the half-life of parathion in estuarine water at room temperature and pH 7.8 is over 218 days.[31] Our experiments at 70 °C were designed to accelerate the degradation, which was observed to be very slow at 25 °C. Typical ^{31}P NMR spectra of the samples taken at the onset of the experiment and after 2 days at 70 °C are shown in Figure 6.

Signals of parathion and *O,O*-diethyl *O*-hydrogen phosphorothioate (diethylthio phosphoric acid, or DeTPA; major hydrolysis product) are seen at 62.4 and 52.0 ppm, respectively, in all samples taken after 2 days of reaction. In the case of the most reactive species, PAMNa, significant presence of tautomeric degradation products such as phosphorothioic *O,O,S*-acid, phosphorothioic *O,O,O*-acid, *O,S*-diethyl O-(4-nitrophenyl) phosphorothioate and *O,O*-diethyl *S*-(4-nitrophenyl) phosphorothioate (in the range 15−32 ppm) as well as phosphine oxide (0.8 ppm) was observed already after 1−2 days at 70 °C, whereas other tested degrading agents based on functionalized clay (ClayPAMNa) and the original montmorillonite K-10 (Clay) exhibited a very minor (<2 mol %) presence of the degradation products other

Table 1. Kinetic Parameters of Parathion Hydrolysis by Untreated Montmorillonite K-10 (Clay), Pralidoxime in Zwitterionic Form (PAMNa) and Montmorillonite Functionalized by PAM (ClayPAM) and PAMNa (ClayPAMNa)

sample	k_{obs} $(h^{-1})^a$	$\tau_{1/2}$ (days)^b	acceleration factor $(k_{obs}/k_{obs}^{control})$	k'' $(M^{-1}\,h^{-1})^c$
buffer control, 25 °C	8×10^{-5}	361	1	na[d]
Clay untreated, 25 °C	1.4×10^{-4}	214	2	na
ClayPAMNa, 25 °C	8.2×10^{-4}	35	10	0.26
buffer control, 70 °C	1.9×10^{-3}	15	1	na
Clay untreated, 70 °C	7.6×10^{-3}	3.8	4	na
ClayPAM,70 °C	9.0×10^{-3}	3.2	5	2.8
ClayPAMNa, 70 °C	3.2×10^{-2}	0.91	17	8.1
PAMNa, 70 °C	6.2×10^{-2}	0.47	33	4.4

[a] Observed pseudo-first-order rate constant. [b] Half-life. [c] Apparent second-order hydrolysis rate constant. [d] Not applicable.

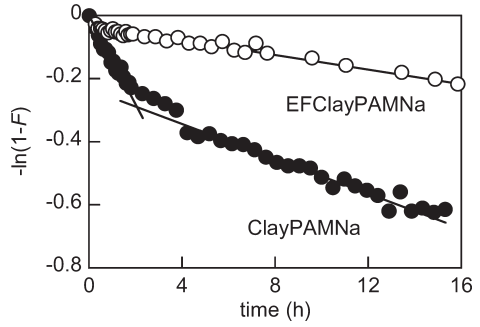

Figure 9. Typical kinetics of DFP degradation on montmorillonite K-10 intercalated with PAMNa (ClayPAMNa) and elastomer film loaded with MMNK-10 intercalated with PAMNa (EFClayPAMNa). Herein, F is the paraoxon conversion (see eq 1). The materials were pre-equilibrated with 100% humidity, at 25 °C. The content of ClayPAMNa in the elastomer film is 26.2 wt %. Solid lines are shown to guide the eye only. The total rotor loading is 50 mg.

than DeTPA after 2 days at 70 °C. Note that the reaction with PAMNa was homogeneous due to the complete dissolution of the oximate in the buffer/acetonitrile solution. The presence of clays made the corresponding reactions to be heterogeneous. In the presence of the oximate, the appearance and increase of the signal corresponding to DeTPA was rapid and steady. The initial stages of degradation were thus predominantly due to the hydrolytic conversion of parathion into DeTPA and were observed to be pseudo-first-order reactions (Figures 7 and 8), as indicated by the linear fit of the curve of $\ln(1 - F)$ vs time (see eq 1), with $R^2 > 0.98$ in all experiments. The slopes of the lines in Figure 7 correspond to the observed reaction rate constant k_{obs}, which is a useful measure of the initial reactivity of our hydrolytic agents.

The corresponding hydrolysis half-life is $\tau_{1/2} = \ln(2)/k_{obs}$. The obtained half-lives are collected in Table 1. Thermogravimetric analysis (Figure 4) enabled estimation of the PAM content in the functionalized clays, and thus the effective initial concentration of the PAM nucleophile (C_{cat}) in the samples of our kinetic experiments was obtained, yielding the apparent second-order hydrolysis rate constant, $k'' = k_{obs}/C_{cat}$[16] (Table 1).

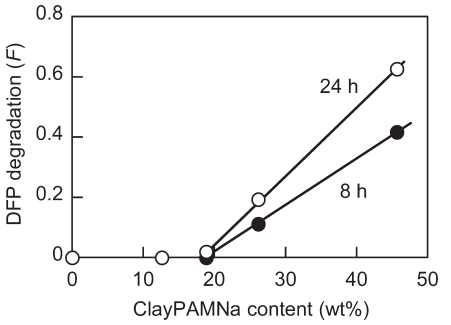

Figure 10. Extent of DFP degradation on elastomeric films containing ClayPAMNa particles on the particle content, after 8 and 24 h of the kinetic experiments. T = 25 °C.

As is seen in Table 1, the pralidoximate indeed accelerated the parathion hydrolysis considerably. The rate enhancement was about 3-fold higher with oximate (PAMNa) compared to the oxime form of PAM, in agreement with our hypothesis of the higher nucleophilicity of the zwitterionic form of PAM. Furthermore, the untreated clay accelerated the hydrolysis, in accord with previous reports,[7,9] but pralidoximate together with clay showed a synergistic effect leading to 3−5-fold higher hydrolysis acceleration than with the untreated clay alone. Of note, the rates of spontaneous hydrolysis measured herein were significantly slower at either 25 or 70 °C than the reported rates in estuarine water at comparable pH,[31] but such a difference can be readily explained by the lower content of water (only 27 wt %) in our experiments.

Diisopropyl Fluorophosphate Degradation. DFP is a close analog of 2-(fluoromethylphosphoryl)oxypropane (sarin) and is widely used in protective material testing to simulate CWA.[16,18] In our experiments, degradation of DFP was tested via deposition of DFP liquid directly onto materials pre-equilibrated with 100% humidity such as functionalized clay as well as elastomeric films modified with functionalized clay. Typical results of the DFP hydrolysis on MMNK-10 intercalated with PAMNa are shown in Figure 9. Notably, the functionalized clay was quite hygroscopic and visibly absorbed water at 100% humidity. The kinetics of the degradation were biphasic in all cases and accelerated with the higher amount of clay loaded into the NMR rotor, as expected. The biphasic nature of the degradation kinetics is probably due to the adsorptive nature of the clay and heterogeneity of the tested DFP-clay system. The DFP droplet deposited onto the clay layer started rapid degradation with the PAMNa molecules available in the immediate proximity, but then the kinetics became transport-limited and slowed down several-fold, due to the DFP permeation through the clay toward unreacted PAMNa sites. The observed rate constants of the initial DFP degradation on MMNK-10 functionalized with PAMNa (oximate loading, 39 wt %) varied in the range 0.14−0.81 h^{-1}, whereas the k_{obs} values estimated from the slope of the curves at $t > 5$ h were in the 0.02−0.03 h^{-1} range. Approximately, 75% of the initial DFP was hydrolyzed on MMNK-10 clay functionalized with PAMNa within a 24 h period, whereas no measurable DFP degradation was observed in identical experiments with untreated MMNK-10 not functionalized by the oximate.

The extent of the DFP hydrolysis by elastomeric films filled by PAMNa-intercalated MMNK-10 particles dramatically depended on the overall content of the particles in the film (Figure.10). PAMNa loadings over 12 wt % of film were

necessary to observe any reactivity. Untreated clay devoid of PAMNa did not show any degradation of DFP within 24 h. All of the functionalized MMNK-10 particles were surrounded by PIB layers, which created a barrier for the reaction at the particle surface, at contents lower than 12 wt %. These data are consistent with the notion of the nonmonotonous dependence of the film reactivity on the content of the reactive component, which needs to be present on the surface for DFP and water accessibility to PAMNa. Once a concentration that leaves PAMNa exposed to the film surface is reached, there is proportionality between the reaction rate and the ClayPAMNa content.

CONCLUDING REMARKS

This work demonstrated that the clay functionalized with an oximate compound is effective in degradation of the OP toxins, including a pesticide and CWA analogue. The clay and the 2-PAM act synergistically, enhancing each other's ability to chemisorb and degrade the OP compounds. It is believed that the functionalized clay is a simple means of creating materials for protective barriers and reactive coatings. Moreover, incorporation of ClayPAMNa (which binds to OP compounds with high efficiency) in an elastomeric film, the main component of the gloves furnished for soldiers and first responders, may address a secondary contamination issue well-known in the chemical agent resistant coatings. When exposed to a chemical agent, the coating will tend to absorb some amount of the agent, and thus there exists a danger that the absorbed agent will be re-emitted, even after decontamination. Even further, since montmorillonite is in the U.S. FDA's Food Additive Database and 2-PAM is an approved drug, their combination through intercalation results in a benign species suitable for applications such as reactive skin decontamination lotions and other decontamination compositions.

ASSOCIATED CONTENT

Supporting Information. HRMAS ^{31}P NMR spectra showing DFP degradation kinetics and ^{1}HNMR spectra of PAM and PAMNA solutions (PDF). This material is available free of charge via the Internet at http://pubs.acs.org/.

AUTHOR INFORMATION

Corresponding Author

*tahatton@mit.edu.

Present Addresses

§Current address: Center for Nanoscale Science and Technology, National Institute of Standards and Technology, Gaithersburg, MD 20899-6203.

ACKNOWLEDGMENT

The authors were supported by the Defense Threat Reduction Agency, in part by Grant HDTRA1-09-1-0012.

REFERENCES

(1) Bhattacharyya, K. G.; Gupta, S. S. *Adv. Colloid Interface Sci.* **2008**, *140*, 114–131.
(2) Rytwo, G.; Nir, S.; Margulies, L. *J. Colloid Interface Sci.* **1996**, *181*, 551–560.
(3) Jaynes, W. F.; Boyd, S. A. *Clays Clay Mine.* **1991**, *39*, 428–436.
(4) Ferrage, E.; Lanson, B.; Sakharov, B. A.; Drits, V. A. *Am. Mineral.* **2005**, *90*, 1358–1374.
(5) Pospišil, M.; Čapková, P.; Weiss, Z.; Maláč, Z.; Šimonik, J. *J. Colloid Interface Sci.* **2002**, *245*, 126–132.
(6) Dios-Cancela, G.; Alfonso-Mėndez, L.; Huertas, F. J.; Romero-Taboada, E.; Sainz-Diaz, C. I.; Hernandez-Laguna, A. *J. Colloid Interface Sci.* **2000**, *222*, 125–136.
(7) Mingelgrin, U.; Saltzman, S. *Clays Clay Miner.* **1979**, *27*, 72–78.
(8) Saltzman, S.; Mingelgrin, U.; Yaron, B. *J. Agric. Food. Chem.* **1976**, *24*, 739–743.
(9) Rav-Acha, C.; Groisman, L.; Mingelgrin, U.; Kirson, Z.; Sasson, Y.; Gerstl, Z. A *Environ. Sci. Technol.* **2007**, *41*, 106–111.
(10) Seger, M. R.; Maciel, G. E. *Environ. Sci. Technol.* **2006**, *40*, 552–558.
(11) Seger, M. R.; Maciel, G. E. *Environ. Sci. Technol.* **2006**, *40*, 791–796.
(12) Seger, M. R.; Maciel, G. E. *Environ. Sci. Technol.* **2006**, *40*, 797–802.
(13) Adams, J. M. *Appl.Clay Sci.* **1987**, *2*, 309–342.
(14) Smolen, J. M.; Stone, A. T. *Environ. Sci. Technol.* **1997**, *31*, 1664–1673.
(15) Moutiers, G.; Le Guével, E.; Villien, L.; Terrier, F. *J. Chem. Soc., Perkin Trans. 2* **1997**, 7–13.
(16) Bromberg, L.; Hatton, T. A. *Ind. Eng. Chem. Res.* **2005**, *44*, 7991–7998.
(17) Shimizu, K.; Higuchi, T.; Takasugi, E.; Hatamachi, T.; Kodama, T.; Satsuma, A. *J. Mol. Catal. A: Chem.* **2008**, *284*, 89–96.
(18) Bromberg, L.; Chen, L.; Chang, E. P.; Wang, S.; Hatton, T. A. *Chem. Mater.* **2010**, *22*, 5383–5391.
(19) Chen, L.; Bromberg, L.; Schreuder-Gibson, H.; Walker, J.; Hatton, T. A.; Rutledge, G. C. *J. Mater. Chem.* **2009**, *19*, 2432–2438.
(20) Terrier, F.; Rodriguez-Dafonte, P.; Le Guével, E.; Moutiers, G. *Org. Biomol. Chem.* **2006**, *4*, 4352–4363.
(21) Tiwari, S.; Kolay, S.; Ghosh, K. K.; Kuca, K.; Marek, J. *Int. J. Chem. Kinet.* **2009**, *41*, 57–64.
(22) Tiwari, S.; Ghosh, K. K.; Marek, J.; Kuca, K. *React. Kinet. Catal. Lett.* **2009**, *98*, 91–97.
(23) Ellin, R. I. *J. Am. Chem. Soc.* **1958**, *80*, 6588–6590.
(24) Nayak, P. S.; Singh, B. K. *Bull. Mater.Sci.* **2007**, *30*, 235–238.
(25) Reddy, C. R.; Bhat, Y. S.; Nagedrappa, G.; Jai Prakash, B. S. *Catal. Today* **2009**, *141*, 157–160.
(26) Jeong, D. W.; Hong, D. S.; Cho, H. Y.; Woo, S. I. *J. Mol. Catal. A: Chem.* **2003**, *206*, 205–211.
(27) Galamboš, M.; Paučová, V.; Kufčáková, J.; Rosskopfová, O.; Rajec, P.; Adamcova, R. *J. Radioanal. Nucl. Chem.* **2010**, *284*, 55–64.
(28) Bongiovanni, R.; Mazza, D.; Ronchetti, S.; Turcato, E. A. *J. Colloid Interface Sci.* **2006**, *296*, 515–519.
(29) Cui, L.; Tarte, N. H.; Woo, S. I. *Macromolecules* **2008**, *41*, 4268–4274.
(30) Rytwo, G.; Nir, S.; Margulies, L. *Soil Sci. Soc. Am. J.* **1996**, *60*, 601–610.
(31) Weber, K *Water Res.* **1976**, *10*, 237–241.